Supporting Information

Metal ions doped carbon dots with strongly yellow photoluminescence

Jian Cheng, Cai-Feng Wang, Yan Zhang, ShengYang Yang, Su Chen*

The quantum yield calculation

The quantum yield measurements were performed with Rhodamine 6G in ethanol (literature quantum yield 0.95 at 488 nm) as the standard. The relative quantum yield values were calculated corresponding to the following equation:

$$\Phi_u=\Phi_s(Y_u/Y_s)(A_s/A_u)(n^2_u/n^2_s)$$

Φ is quantum yield; Y is the measured integrated fluorescence emission intensity; A is the optical density measured at the excitation wavelength; n is the refractive index. The subscript "s" refers to the standard. The subscript "u" refers to the unknown quantum yield of Zn^{2+}-doped CDs. The refractive indexes of water and ethanol were 1.333 and 1.362, respectively (the CDs aqueous solutions were assumed as water). In order to minimize re-absorption effects, absorbance were kept under 0.05.

Table 1 Quantum yield measurements of Zn^{2+}-doped CDs.

	Φ_s	Y	A	n	Φ_{CD}
Rhodamine 6G	0.94	3106	0.042	1.362	51.2%

Fluorescence lifetime calculation

The fluorescence lifetime (τ) of CDs was assessed by time-resolved photoluminescence measurements. The decay trace for CDs was fitted using biexponential functions Y(t) based on non-linear least squares analysis in Equation (1)

$$Y(t)=\alpha_1\exp(-t/\tau_1)+\alpha_2\exp(-t/\tau_2) \quad (1)$$

Where α_1 and α_2 are the fractional contributions of timeresolved decay lifetime of τ_1 and τ_2. According to Equation (2),

$$\overline{\tau} = \frac{\alpha_1\tau_1^2 + \alpha_2\tau_2^2}{\alpha_1\tau_1 + \alpha_2\tau_2} \quad (2)$$

we calculated the average lifetime $\bar{\tau}$ of Zn^{2+}-doped CDs as 6.8 ± 0.05 ns. The chi-squared (χ^2) values of the fittings were maintained below.

Table 2 Fluorescence lifetimes of Zn^{2+}-doped CDs and Without Zn^{2+}-doped CDs.

	$\alpha_{1(\%)}$	$\tau_{1(ns)}$	$\alpha_{2(\%)}$	$\tau_{2(ns)}$	χ^2
Zn^{2+}-doped CDs	78.7	2.6	21.3	10.6	0.99
Without Zn^{2+}-doped CDs	63.8	4.5	36.2	6.7	1.05

Figures:

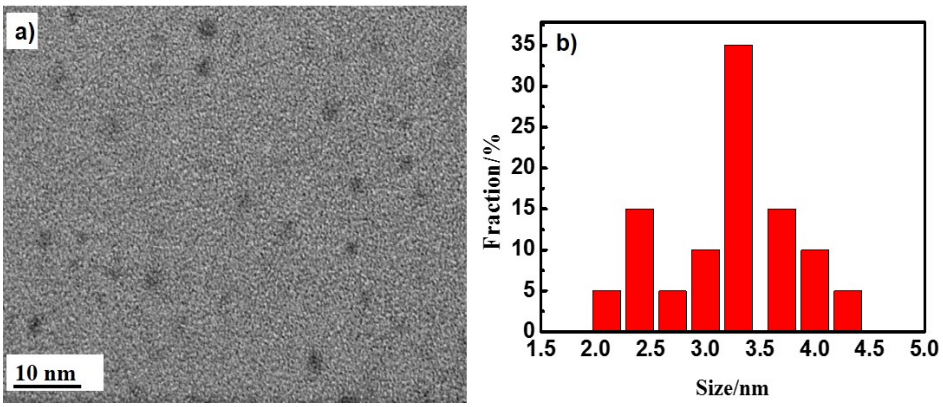

Fig. S1 a) TEM image of Zn^{2+}-doped CDs. b) Size histogram of Zn^{2+}-doped CDs derived from TEM image in Fig. S1a.

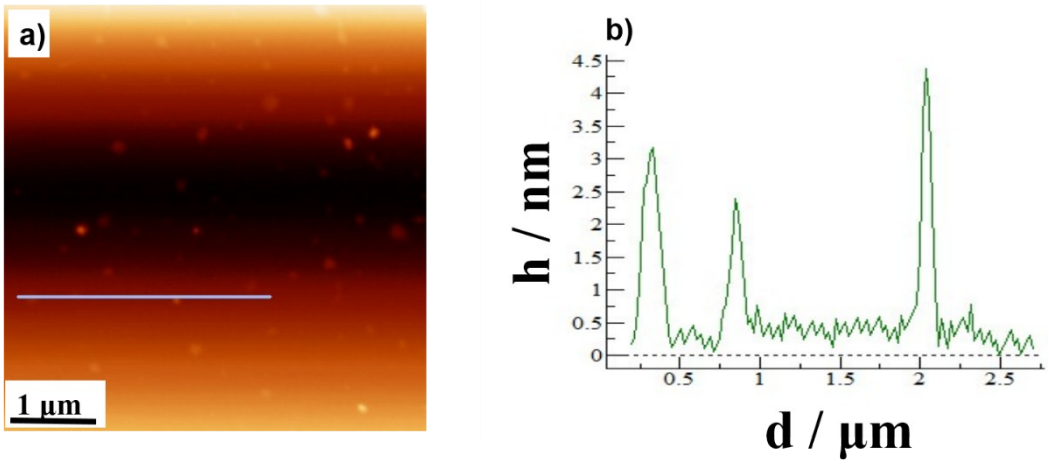

Fig. S2 a) AFM topography image of Zn^{2+}-doped CDs on mica substrate. b) With the height profile analysis along the line in the image.

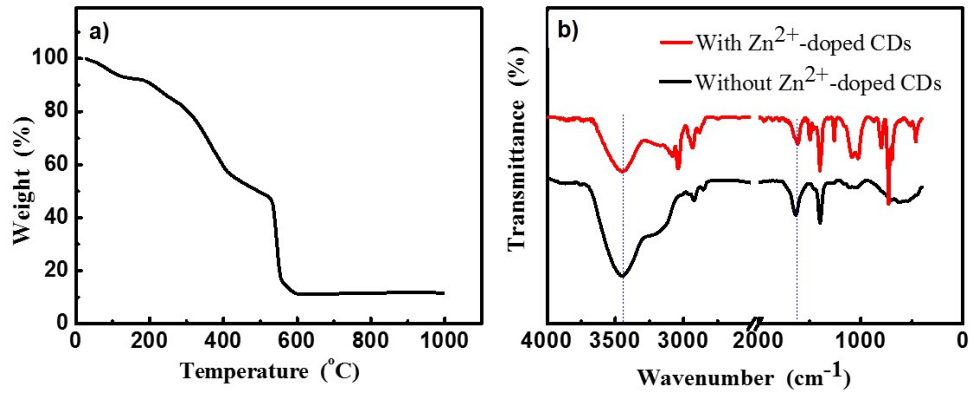

Fig. S3 a) TGA image of the Zn^{2+}-doped CDs (10°C min^{-1} in air flow). b) FTIR spectra of the Zn^{2+}-doped CDs (red) and without Zn^{2+}-doped CDs (black).

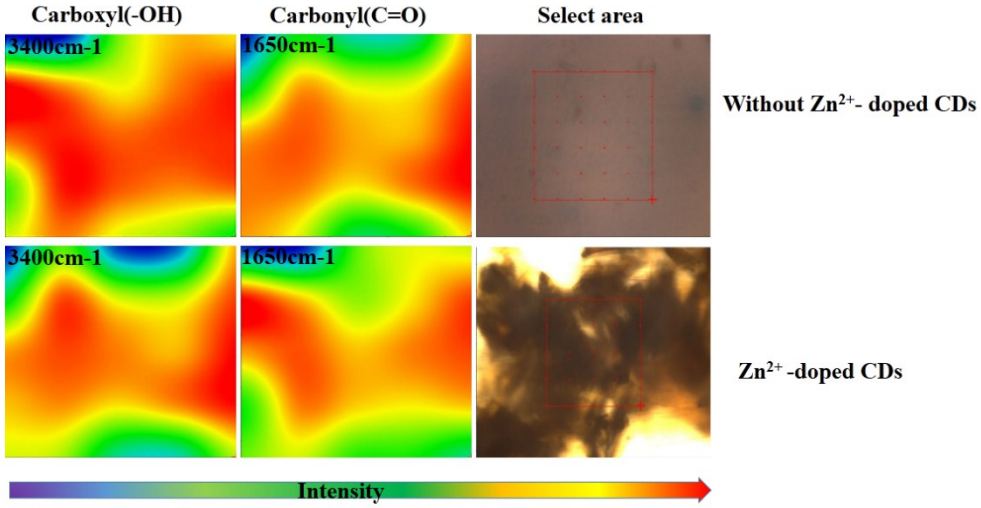

Fig. S4 MFTIR spectra of carboxyl (3400 cm^{-1}) and carbonyl (1650 cm^{-1}) groups of without Zn^{2+}-doped and CDs Zn^{2+}-doped CDs.

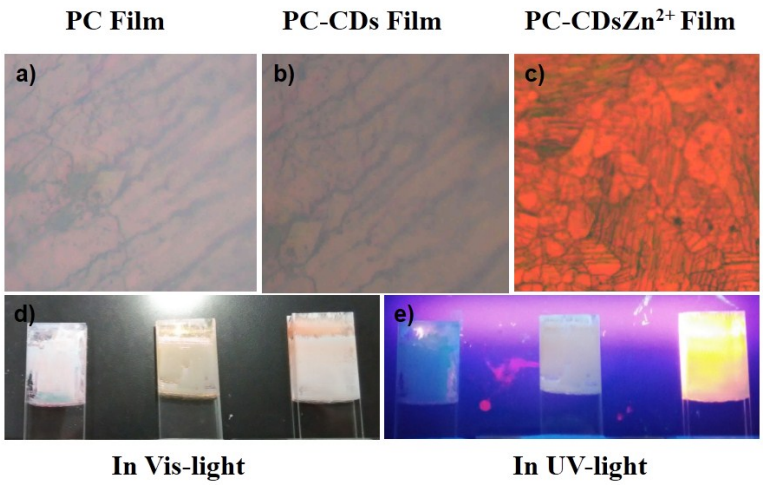

Fig. S5 a) Structural color of a) PC film, b) PC-CDs film and c) PC-CDs_{Zn}^{2+} film by the Metallurgical Microscopy., Images of PC film, PC-CDs film, PC-CDs_{Zn}^{2+} film under Vis-light d) and UV-light e), respectively.

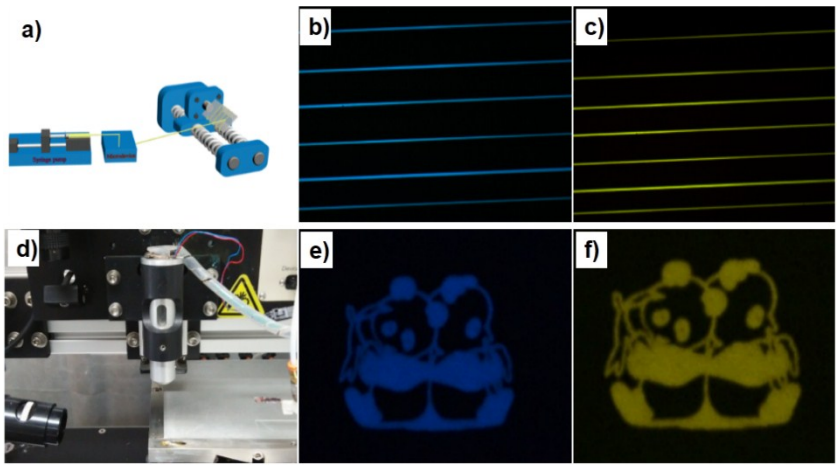

Fig. S6 a) Scheme diagram of the microfluidic-spinning device. b), c) Fluorescence microscopy images of CDs–PVP fluorescent microfibers under UV light (Without Zn^{2+}-doped CDs (b) and Zn^{2+}-doped CDs (c)). d) Nano inkjet printer. Fluorescent patterns with CDs (Without Zn^{2+}-doped CDs (e) and Zn^{2+}-doped CDs (f))